Published in the Proceedings of the Fourth Conference on Electromagnetic and Light Scattering by Nonspherical Particles. Theory and Applications, held in Vigo, Spain, September 20-21, 1999.

Polarized light scattering measurements of roughness, subsurface defects, particles, and dielectric layers on silicon wafers

Thomas A. Germer[a] and Lipiin Sung[a,b]

[a]*National Institute of Standards and Technology, Gaithersburg, MD 20899*
[b]*University of Maryland, College Park, MD 20742*

This article outlines theoretical and experimental results for polarized light scattering from five different sample configurations: surface roughness of a single interface, defects below a single interface, spherical particles above a single surface, spherical particles above a dielectric film, and roughness of the top interface of a dielectric film. These measurements demonstrate that polarized light scattering can be used to characterized defects on surfaces, provided sufficient information is available about the system without defects. It is found that measurement of the principal direction of the polarization for *p*-polarized incident light, $\eta^{(p)}$, when measured out of the plane of incidence, can be used to distinguish amongst light scattered by microroughness, subsurface defects, and particulate contaminants.

I. INTRODUCTION

Measurements of scattered light are often used to inspect the quality of smooth surfaces.[1] Usually, a laser beam is allowed to impinge on the sample of interest, and one or more optical elements collect light onto a highly sensitive detector. These techniques offer high sensitivity to many types of defects, including roughness, subsurface features, and particulate contaminants. However, it is often difficult to distinguish amongst these various scattering mechanisms, especially if only a small number of detectors are employed by the instrumentation. Furthermore, the sensitivity to local defects is often limited by non-localized scattering resulting from roughness of the sample and Rayleigh scattering in the air.

Ultimately, instrumentation which can perform "on the fly" characterization of defects is needed. These tools need not only to detect defects, but also to classify them according to type, size, material, and shape. With traditional light scattering techniques, this can be partially achieved by using multiple scattered light detectors, each which views the sample scattering region from a direction optimized for scattering from a specific type of defect. This technique, however, is limited to being able to distinguish between only a small number of defect types.

Recent studies have found that when *p*-polarized light is incident on a sample at an oblique angle of incidence, the light scattered by that sample has a polarization that is dependent upon the nature of the scattering source.[2,3] Furthermore, it has been found that light scattered by small amounts of interfacial roughness has a polarization that is independent of the details of that roughness, such as the power spectral density function of

the surface height function or the absolute magnitude of that roughness.[4] Using that finding, it has been possible to develop tools which are "blind" to roughness, while maintaining sensitivity to other sources of scattering.[5] These polarized light scattering techniques should substantially extend the capabilities of light scattering inspection tools.

This article will review the results of experimental and theoretical studies that demonstrate how the polarization of scattered light can offer a means for distinguishing amongst different scattering sources. In Sec. II, the bidirectional ellipsometry (BE) method that we use to partially characterize the scattered light will be outlined. In the following four sections, examples will be given for microroughness of a single interface (Sec. III), subsurface features (Sec. IV), particles above a single interface (Sec. V), particles above a dielectric layer (Sec.VI), and roughness of an interface in a dielectric film (Sec. VII). In Sec. VIII, the results will be summarized.

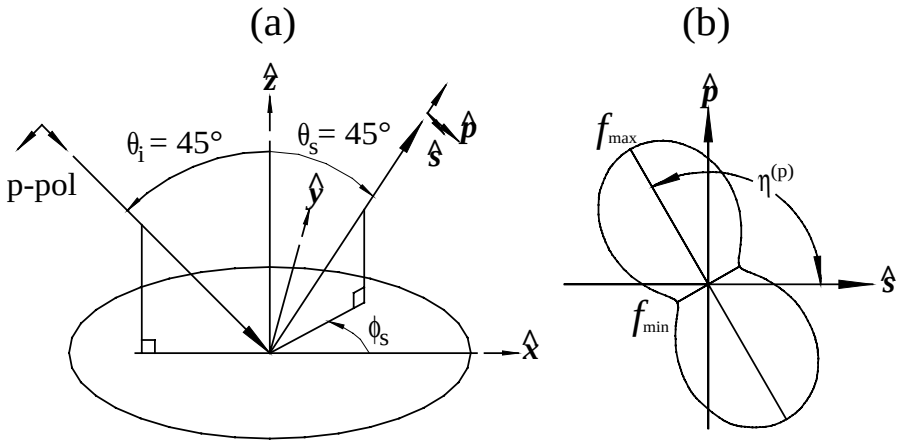

FIGURE 1 (a) The sample coordinate system used in this paper; and (b) a schematic of the intensity distribution f measured by a rotating linear-polarization-sensitive detector, defining the bidirectional ellipsometry parameters, $\eta^{(p)}$ and $P_L^{(p)} = (f_{max} - f_{min})/(f_{max} + f_{min})$.

II. BIDIRECTIONAL ELLIPSOMETRY

Figure 1(a) outlines the measurement geometry used in this study. Laser light of wavelength $\lambda = 532$ nm and *p*-polarization (electric field within the plane of incidence) is incident onto a sample at an angle $\theta_i = 45^o$. The light scattered into a small solid angle Ω in the direction defined by a polar angle $\theta_s = 45^o$ and an azimuthal angle ϕ_s is collected by a rotating polarization-sensitive detector. Figure 1(b) illustrates schematically the signal one obtains as the detector polarization direction is rotated. Bidirectional ellipsometry (BE) parameters, consisting of the principal direction of the polarization, $\eta^{(p)}$, and the degree of linear polarization, $P_L^{(p)}$, are recorded as functions of ϕ_s for fixed θ_i and θ_s. This out-of-plane scattering geometry is designed to optimize the distinction between the different scattering mechanisms. If measurements were carried out only in the plane of incidence, contrast would only be obtained amongst mechanisms if a mixture of *s*- and *p*-polarized light were used, e.g. 45º or circularly polarized light. However, theoretical calculations have shown that scattering from (or

scattering into) *s*-polarized light is relatively independent of scattering mechanism.[2] Therefore, out-of-plane measurements of the polarization with *p*-polarized incident light provides the greatest contrast amongst mechanisms.

The experimental method used to perform BE measurements is outlined in detail elsewhere.[6] The goniometric system is of a relatively simple design, having the incident laser beam fixed with respect to the laboratory, the scattered light receiver moving horizontally about a single vertical axis, and the rest of the necessary degrees of freedom being achieved through sample rotations and translations. The control of the goniometer with respect to sample-specific coordinates (e.g. θ_i, θ_s, ϕ_s, and the incident and scattering polarizations) is performed by a computer. This system is of a design that should be easily replicated elsewhere for light scattering measurements.

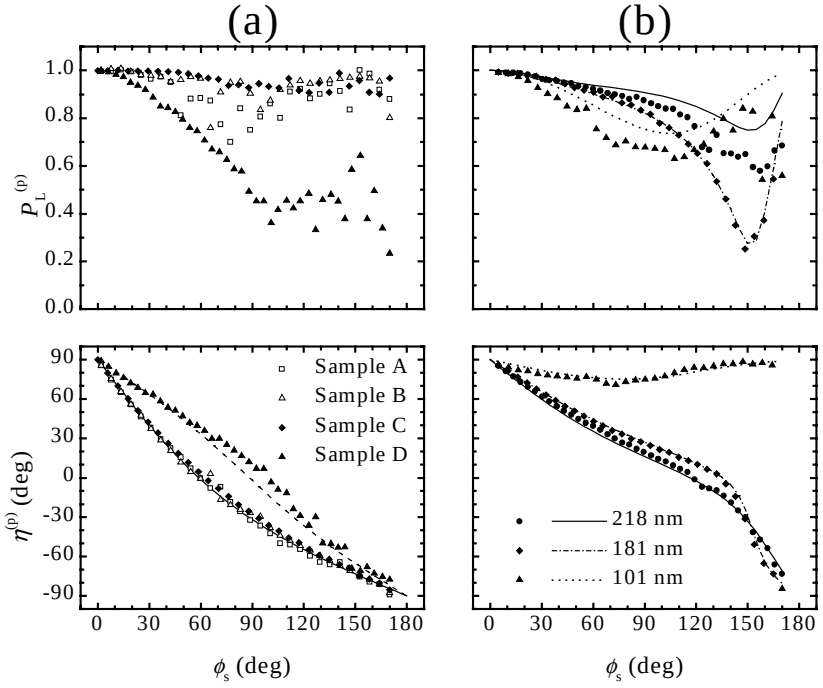

FIGURE 2 BE parameters, experimental and theoretical, (a) for four different silicon samples, and (b) for different size PSL spheres deposited on silicon.

III. MICROROUGHNESS

Figure 2(a) shows the results of BE measurements from four different silicon samples.[7] The first two samples, Samples A and B, were pseudorandom two-dimensionally rough surfaces, generated by a photolithography process.[8] The surfaces consist of pseudorandom distributions of 1.31 μm and 1.76 μm diameter pits having nominal depths of 1 nm and 10 nm, respectively, with one pit of each diameter for every 5 $\mu m \times 5$ μm square on the surface. Sample C consisted of an etched backside of a wafer, which exhibited a high degree of scattering and a very weak specu-

lar reflection. Samples A, B, and C should all scatter by varying levels of surface topography. Sample D, in contrast, contains subsurface defects and will be discussed in Sec. IV.

The curves shown in Fig. 2(a) represent the results of first-order vector perturbation (Rayleigh-Rice) theory. This theory assumes that the sample consists of an interface between the substrate material and the ambient air, with the boundary being given by a surface height modulation function, $z(x,y) = z_0 + \Delta z(x,y)$. The function $\Delta z(x,y)$ is assumed to be single valued, to be small compared to the wavelength of the probing light, to have zero mean, and to have slopes much smaller than unity. Under these conditions, the electromagnetic fields and the surface normal can be expanded about their zero-order values. The condition that the electric and magnetic fields parallel to the surface must be continuous across the boundary allows one to calculate the first-order scattered field. The agreement between the experimental data and the theoretical predictions in Fig. 2(a) is very good.

An interesting feature of the first-order solution is the separation between those terms affecting the polarization and those containing the function $\Delta z(x,y)$. That separation indicates that the entire class of microrough surfaces can be identified by BE measurements, despite the presence of random variables in $\Delta z(x,y)$. It also allows one to collect light scattered into any direction and to eliminate with a polarizer any signal that can potentially result from microroughness. If the scattered signal noise is dominated by microroughness, this method allows one to substantially increase their sensitivity to other sources of scattering, such as subsurface defects and particulate contamination.

IV. SUBSURFACE DEFECTS

Figure 2(a) also shows the BE parameters measured for a silicon sample, Sample D, having a high concentration of "crystal originated particles," or COPs, which are SiO_2 precipitates in the bulk material.[9] These defects gained their misnomer, since they would be detected as light scattering events by some instruments and therefore counted as particles. It is clear from Fig. 2(a) that these defects have BE parameters significantly different from those for roughness, and will be shown in Sec. V to be different from those for particulate contamination.

One of the curves shown in Fig. 2(a) is the result of calculations based upon the Rayleigh approximation. In this approximation, the defects are assumed to be small enough that one can treat them as point polarizable dipoles. The local electric field, which for *p*-polarized incident light is nearly parallel to the surface, defines the direction of the induced dipole moment. This induced dipole moment then radiates as an antenna from below the surface. The finite size and shape of the defect and any secondary interactions (near-field or far-field) are ignored in this approximation. The agreement between the measured BE parameters and this theory, despite the crudeness of the approximation, is very good.

Other BE measurements have been performed for known subsurface features, using transparent materials having known bulk scattering behav-

iors, and the agreement has been very good.[3] It was found that even high-level scatterers, such as glass ceramics, show excellent agreement with the Rayleigh theory for the parameter $\eta^{(p)}$, despite having very poor agreement for $P_L^{(p)}$. This finding is not unexpected, since materials such as these are expected to exhibit a high degree of depolarization due to multiple scattering and finite-domain-size effects. The parameter $\eta^{(p)}$, however, is much more robust, since it is less sensitive to the exact nature of the scatterer than to the local mean field at the scatterer. Simple symmetry arguments dictate that a statistically spherically-symmetric scatterer will scatter primarily in a Rayleigh-like fashion, albeit with some depolarization, which results from the ensemble averaging of the random configurations.

V. SPHERICAL PARTICLES ABOVE A SINGLE INTERFACE

While the electric field amplitude below a single interface is constant (with the light incident from above), the amplitude and direction of the field above the interface varies with *z*-coordinate due to interference between the incident and reflected light. That fact leads to most of the success for the characterization of subsurface defects given in Sec. IV, and also provides the ability to locate particles above a surface. For a single interface, this location is directly correlated with the size of a particulate contaminant.

Figure 2(b) shows BE results for high surface densities of three diameters (101 nm, 181 nm, and 218 nm) of polystyrene latex (PSL) spheres deposited onto bare silicon wafers.[10] It can be seen from Fig. 2(b) that each sphere diameter yields a unique BE curve, allowing one to distinguish one diameter sphere from another. The curves, shown in Fig. 2(b), are the results of calculations based upon the discrete dipole approximation (DDA). In the DDA, an object is built from a large number of interacting dipoles. The near-field interactions between successive dipoles, both directly and through their reflections in the surface, are included in the calculation. A self-consistent solution for all the dipoles is iteratively determined. A complete description of the DDA algorithm is given elsewhere.[11]

The agreement between the DDA calculations and the experimental data is very good. Small deviations between the theory and experiment for the 101 nm spheres are understood as resulting from a fraction of the deposited particles being doublets, while small depolarization (reduction in $P_L^{(p)}$) from the 218 nm spheres probably results from their imperfect sphericity.[10] Any scattering mechanism whose polarization is dependent upon some parameter will partially depolarize light if that parameter has a finite width distribution. The light scattered by a doublet or a non-spherical particle, for example, has a polarization that depends upon its orientation.

Although we use the DDA method to calculate the light scattered by a sphere above a surface, we also compare the DDA method to simpler and less accurate approximations.[10] In the Rayleigh approximation, outlined above in Sec. IV, the only parameter which determines the polarization of

the scattered light is the mean distance of the sphere from the surface. In the Mie-surface approximation (sometimes referred to as the double interaction model[12]), we include the field scattered by a homogeneous sphere, using the exact Mie solution for a sphere in free space, therefore taking into account the finite size and material of the sphere. Both of these approximations ignore the sphere-surface near-field interaction, yet they provide insight into which parameters are most important at determining the polarization of scattered light. It is found that for small scattering angles ($\phi_s \leq 60^o$), that all three approximations yield very similar results for the BE parameter $\eta^{(p)}$. This finding indicates that the parameter that affects $\eta^{(p)}$ for these small angles is primarily the mean distance that the particle lies from the surface, and allows one to determine particle size independent of particle material. For nearly-spherical particles, the parameter $\eta^{(p)}$ at small scattering angles should still allow one to make an estimate of contaminant size.

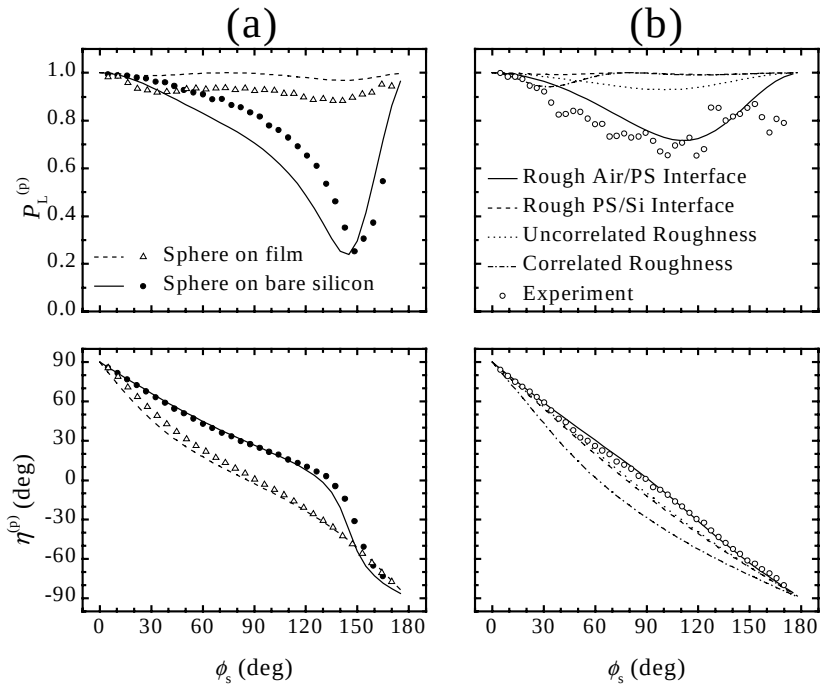

FIGURE 3 BE parameters, experimental and theoretical, (a) for 181 nm PSL spheres deposited on a 55 nm PS film, and (b) for roughness in a 55 nm PS film deposited on silicon.

VI. SPHERICAL PARTICLES ABOVE A DIELECTRIC LAYER

Figure 3(a) shows the scattering from 181 nm PSL spheres deposited onto a 55 nm thick polystyrene (PS) layer spin-cast onto a silicon wafer. These results are compared to those for 181 nm PSL spheres deposited directly onto bare silicon. The theoretical calculations, based upon the Mie-surface approximation, are included in Fig. 3(a), and include the multiple reflections in the dielectric layer. The agreement between the theory and experiment is very good. The less than ideal agreement between the calculations and the data for the spheres on bare silicon is due to

the neglect of the near-field interaction in this theory. (Our current implementation of the DDA code does not account for dielectric layers.)

The presence of the dielectric layer has a pronounced effect on the BE parameters for identically-sized spheres. This finding is in agreement with our understanding that the particle effectively samples the local field a distance from the surface given by the radius of the particle, and radiates from that same position. The presence of the dielectric layer affects the reflection coefficients of the substrate, upon which the particle lies. It is therefore necessary that the substrate and film optical constants and film thickness be known in order to determine the particle size. This information can be obtained from specular ellipsometry.

VII. ROUGHNESS OF A DIELECTRIC LAYER

The 55 nm PS film shown in Fig. 3(a) has some residual roughness before spheres were deposited on it. The resulting scattered light was about twenty times less intense than that from the spheres, and about an order of magnitude greater than the scattering from the bare wafer before deposition of the film. Figure 3(b) shows the BE parameters for this film, compared to the results of four calculations based on first-order vector perturbation theory, outlined above, accounting for the presence of the dielectric layer.[13] The four calculations correspond to roughness of the air/PS interface, roughness of the PS/silicon interface, identical but uncorrelated roughness of both interfaces, and identical and correlated roughness of both interfaces. The good agreement between the data and the calculations for a rough air/PS interface are consistent with the larger degree of scattering from this system, compared to that of the bare silicon wafer, and with atomic force microscopy (AFM) images of the films.

VIII. SUMMARY

The results of BE measurements given in this paper demonstrate that different sources of scattering can often be distinguished from one another by observing the polarization of the scattered light. In all of these cases, information about the ideal system, such as the optical constants for the substrate and any films, and the thickness of those films, is necessary as accurate parameters to theoretical models. Measurement of the polarization of scattered light ought to be incorporated into inspection instruments in order to improve the capability for rapid classification of defects.

ACKNOWLEDGEMENTS

The authors would like to thank Dr. George Mulholland of NIST for assistance in the particle depositions, and Bradley Scheer of VLSI Standards, Inc. for providing the photolithograhically-generated microrough silicon samples.

REFERENCES

[1]J. C. Stover, *Optical Scattering: Measurement and Analysis*, (SPIE Optical Engineering Press, Bellingham, WA, 1995).

[2]T. A. Germer, "Angular dependence and polarization of out-of-plane optical scattering from particulate contamination, subsurface defects, and surface microroughness," Appl. Opt. **36**, 8798–8805 (1997).

[3]T. A. Germer and C. C. Asmail, "Polarization of light scattered by microrough surfaces and subsurface defects," J. Opt. Soc. Am. A **16**, 1326–1332 (1999).

[4]T. A. Germer, C. C. Asmail, and B. W. Scheer, "Polarization of out-of-plane scattering from microrough silicon," Opt. Lett. **22**, 1284–1286 (1997).

[5]T. A. Germer and C. C. Asmail, "Microroughness-blind hemispherical optical scatter instrument," U.S. Patent Application #09/058,182 (April 10, 1998).

[6]T. A. Germer, and C. C. Asmail, "A goniometric optical scatter instrument for bidirectional reflectance distribution function measurements with out-of-plane and polarimetry capabilities," in *Scattering and Surface Roughness,* eds. Z.-H. Gu and A. A. Maradudin, Proc. SPIE **3141**, 220–231 (1997); T. A. Germer and C. C. Asmail, "Goniometric optical scatter instrument for out-of-plane ellipsometry measurements," Rev. Sci. Instrum, in press.

[7]The uncertainties in the reported results are dominated by statistical sources and are typically smaller than the size of the symbols used in the graphs or the statistical spread in the data from point to point, whichever is larger.

[8]B. W. Scheer, "Development of a physical haze and microroughness standard," in Flatness, Roughness, and *Discrete Defect Characterization for Computer Disks, Wafers, and Flat Panel Displays*, ed. J. C. Stover, Proc. SPIE **2862**, 78–95 (1996).

[9]J. Ryuta, E. Morita, T. Tanaka, and Y. Shimanuki, "Crystal-originated singularities on Si wafer surface after SC1 cleaning," Jpn. J. Appl. Phys. **29**, L1947–L1949 (1990).

[10]L. Sung, G. W. Mulholland, and T. A. Germer, "Polarization of light scattered by particles on silicon wafers," in *Surface Characterization for Computer Disks, Wafers, and Flat Panel Displays*, ed. J. C. Stover, Proc. SPIE **3619**, 80–91 (1999); L. Sung, G. W. Mulholland, and T. A. Germer, "Polarization of light scattered by spheres on silicon," Opt. Lett., in press.

[11]R. Schmehl, B. M. Nebeker, and E. D. Hirleman, "Discrete-dipole approximation for scattering by features on surfaces by means of a two-dimensional fast Fourier transform technique," J. Opt. Soc. Am. A **14**, 3026–3036 (1997).

[12]K. B. Nahm, and W. L. Wolfe, "Light-scattering models for spheres on a conducting plane: comparison with experiment," Appl. Opt. **26**, 2995–2999 (1987).

[13]T. A. Germer, "Application of bidirectional ellipsometry to the characterization of roughness and defects in dielectric layers," in *Flatness, Roughness, and Discrete Defect Characterization for Computer Disks, Wafers, and Flat Panel Displays II*, ed. J. C. Stover, Proc. SPIE **3275**, 121–131 (1998).